Finite element models in the steel industry

Part II: analyses of tubular products performance

Eduardo N. Dvorkin[*] *and Rita G. Toscano*

Center for Industrial Research, FUDETEC
Av. Córdoba 320
1054 Buenos Aires, Argentina

Abstract

In this paper we discuss the finite element models that we developed for simulating the service performance of the tubular steel products used in the oil industry. These tubular products include the oil country tubular goods (OCTG), that is to say the tubular products used in the oil wells, and the pipes used in pipeline applications.

1. Introduction

The failure of pipes used in the oil industry either for well applications, as in the case of the oil country tubular goods (OCTG) shown in Fig. 1, or for transporting oil and gas, as in the case of pipelines, usually involve ecological hazards and important revenue loses.

Pipes may fail either due to corrosion or to thermo-mechanical loads outside the allowable loads envelope. Considering the social and economical impacts of the pipes mechanical failure, it is fundamental to have reliable evaluations of their strain / stress state under different service conditions and of their allowable loads envelope.

In this paper we discuss the finite element models that we developed for simulating the service performance of the tubular steel products used in the oil industry. In particular we will concentrate on the analysis of threaded connections for OCTG and on the analysis of the collapse pressure of pipe bodies (OCTG and pipelines).

Failure of threaded connections

The threaded connections used to join the pipes belonging to the casing or to the tubing (Fig. 1) can be classified in two groups:

- Connections covered by the API standards, such as the API 8-Round connection or the Buttress connection [1] (see Figs. 2.a and b). The main function of these connections is structural, even tough they provide some liquid or gas sealing-barrier between the pipe internal and external volumes [2].
- Premium connections (see Fig. 2.c), in addition to their structural function they provide a gas sealing-barrier between the pipe internal and external volumes.

[*] Corresponding author. E-mail: dvk@siderca.com

When dealing with premium connections we recognize two different failure modes: the *structural failure* and the *functional failure*.

We can recognize the following failure modes for threaded connections:

a. Jump-out: in Fig. 3 [2] we indicate in an API 8-Round connection the levels of equivalent plastic strain for different tensile loads and we show the development of the jump-out phenomenon.

b. Localized plastic deformation: in Fig. 4 we present a finite element simulation of a casing premium connection necking, notice that the failure is localized out of the threaded area. In the same figure we also indicate the load-displacement path, for two different thread shapes that have an identical performance.

c. Rupture of the pipe material without the development of large plastic strains: in Fig.5 we present a photograph of a tubing premium connection that failed in the threaded area.

The metal-to-metal seal indicated in the premium connection in Fig. 2.c may also fail in preventing a gas or liquid from leaking; this is a connection functional failure.

Usually finite element analyses are very successful in providing a detailed picture of the stresses / strains in a connection under a specific loading, including the contact stresses in the metal-to metal seal [3-5]. However, there is still not enough available knowledge to theoretically predict, from the seal contact stresses, the sealing capability of a connection.

Collapse failure

Steel deep-water pipelines under external pressure plus bending may reach their load carrying capacity due to two failure modes:

- Global buckling [6,7]: in this case the pipeline buckles in a *"column mode"*.
- Localized collapse [8,9]: in this case the pipe structure collapses with its sections loosing their round shape (see Fig. 6)

In the design of marine pipelines it is very important to determine the collapse pressure of steel pipes subjected to external hydrostatic pressure and bending. It is fundamental to be able to quantify the effect of manufacturing imperfections such as ovality, eccentricity and residual stresses on the collapse pressure [9].

The tracking of the post-collapse equilibrium path is also necessary to be able to assess on the stability of the post-collapse regime; that is to say, in order to assess if a collapse will be localized in a section or will propagate along the pipeline [10]. Hence, it is also fundamental to analyze the effect of the geometrical imperfections and of the residual stresses on the collapse propagation pressure, which is the lowest external pressure that will propagate the collapse along the pipeline, for a constant applied curvature [11].

In the second section of this paper we discuss on the modeling of OCTG threaded connections and in the third section we discuss on the modeling of the collapse and post-collapse behavior of pipes.

2. Modeling of OCTG Threaded Connections

The performance analysis of OCTG premium connections using finite element models is nowadays progressively replacing the use of full-scale tests in the design phase of new connections and has been incorporated, in proper combination with full-scale tests, in the qualification procedure of existing connections.

In full-scale tests it is usually difficult to identify the causes behind structural or functional failures, even if extensive strain-gauging instrumentation is used; many times unidentified connection manufacturing errors mask the test results. Finite element models on their side are very suitable for making parametric analyses in which the influence of different design parameters on the connection performance can be identified. On the other hand, while finite element models can accurately predict the structural failure loads and failure modes of connections (e.g. jump-out, necking, etc.) they can only provide qualitative indications about the functional failure of connections.

Since finite element models are increasingly being used as engineering tools in the evaluation process of premium connections performance, it is important that their results are reliable. The main features that a finite element formulation used for the analysis of threaded connections has to include are [3]:

- Material and geometrical nonlinear analysis capabilities [12]. The finite element result displayed in Fig. 4 was obtained with an analysis that incorporated contact conditions and finite strains elasto-plasticity.
- Realistic elasto-plastic material models; e.g. a von Mises material model with either isotropic or kinematic hardening [12].
- A contact algorithm able to represent large sliding situations between the surfaces in contact [12]. Node-to-node contact algorithms are not good enough, as can be seen in the example presented in Fig. 3.
- Efficient iteration techniques [12,13].
- Reliable axisymmetric element formulations (normally OCTG connections are analyzed using axisymmetric models)

The main requirements for a reliable 2D finite element formulation are [5,14,15]:

- Non-locking behavior (the commonly used standard 4-node isoparametric element locks).
- No inclusion of spurious zero energy modes (the under integrated 4-node isoparametric element includes zero energy modes).
- Satisfaction of Irons Patch Test (guarantees convergence even tough this convergence may be slow) [12,16,17].
- Low sensitivity to element distortions. In a standard mesh, such as the one shown in Fig. 7, quite distorted elements need to be used. Quadrilateral elements having only "exterior degrees of freedom" cannot be strictly insensitive to distortions if the Patch Test is to be satisfied [18]; hence, we have to require in the element formulation the strict satisfaction of the Patch Test and as less sensitivity to elements distortions as possible.
- Ability to capture shear bands without unrealistic diffusion of the plastic deformation zone [5]. This is an important requirement since the failure modes during overtorque,

compression or external pressure develop shear bands in the connection coupling (see Fig. 8).

Our QMITC quadrilateral element [5,14,15] satisfies the above requirements and therefore it is our standard element for analyzing OCTG threaded connections.

Once a finite element formulation has been selected and connection models have been developed, it is important to compare the model predictions with strain-gauge measurements performed in full-scale tests. In previous references [4,5] the results obtained using the QMITC element, implemented in the general-purpose finite element code ADINA [19], were compared with the results obtained during full-scale tests, getting an excellent matching.

2.1. Sealability analysis

As we discussed above it is yet not possible to produce a quantitative assessment on the sealability of a connection from the contact stresses in the metal-to-metal seal. However, in order to be able to compare the potential for sealability of different seal designs we have defined three *"sealability indicators"*:

Seal length (LS)

It is the length of the metal-to-metal seal on which the contact pressures are larger than the pipe internal pressure.

LP2 indicator

Using the results of the finite element models we calculate:

$$LP2 = \frac{1}{2\pi}\int \langle \sigma_{cc} - ip \rangle ds$$

where σ_{cc} are the seal contact stresses and *ip* is the internal pressure.

The Macauley bracket $\langle x \rangle$ is defined as:

$$\langle x \rangle = \{ x \quad for \quad x \geq 0 \quad or \quad 0 \quad for \quad x < 0 \}$$

LP∞ (peak contact stress) indicator

Is the maximum value of the contact stress along the seal area.

In Fig. 9, as an example, we plot the contact pressures developed in two different metal-to-metal seals: a cone-to-cone seal and a cone-to-sphere seal; for both cases we indicate the above defined sealability indicators. The cone-to-cone design presents a larger value of LP_∞, while the sphere-to-cone presents a larger value of *LS*; it is not obvious which one of the two designs offers a better sealability for gas; only full-scale sealability tests with gas pressurization can answer the above question.

In order to illustrate on the prediction capabilities of different element formulations in Fig. 10 we present for a cone-to-cone seal the contact pressure distributions predicted by the QMITC and Q1-P0 elements; the QMITC formulation can capture larger stress gradients.

2.2. Validation of finite element results using full-scale tests

In previous publications [3,4] we compared the finite element predictions for strains (axial and hoop strains) in pin and box of different premium connections with strain-gauge measurements performed, under different loading conditions, during full-scale tests. In those publications we showed that the agreement between the numerically determined and experimentally determined strains was excellent.

It is well known that if during the connection make-up, too much dope is used either in the seal area or in the thread area, the extra dope gets trapped and develops a high pressure that can damage the connection. Of course, different connection designs have more or less capability for avoiding the dope trapping.

A connection similar to the one shown in Fig. 7 was made-up with extra dope and the dope pressure values shown in Fig. 11 were measured during the make-up. In Fig. 12 we compare the strains determined via a standard finite element analysis with the strains measured in the full-scale test; it can be seen that the agreement between numerical and experimental values is not as good as in the cases reported in our previous publications. Then we re-run the analysis adding among the loads the dope pressure distribution determined in the full-scale test, in Fig. 13 we compare the experimental results with the numerical results with and without the inclusion of the dope pressure; it is obvious that the inclusion of the dope pressure improves the matching between the experimental and numerical results.

2.3. Results obtained for a steam injection string

The behavior of a connection in a steam injection string is simulated in this subsection. In Fig. 14 we present the thermal and mechanical loads considered for the analysis and the results are shown in Figs. 15 and 16.

From the equivalent plastic strain and contact pressure plots it is evident that successive cycles do not produce ratcheting in the connection.

3. Modeling of tubular products collapse

In a previous publication [9] we presented finite element models that we developed for studying the collapse behavior of steel pipes under external pressure; in that publication we also presented the validation of our numerical models by comparing their predictions with the results of laboratory collapse experiments.

Our purpose in the present section is to extend the study to the post-collapse regime and to loading cases that combine external pressure and bending [11].

3.1. The finite element models

In this sub-section we discuss the numerical models we implemented to simulate the behavior of a very long pipes (infinite tube model) and short pipe samples (finite tube model). Using these models we investigate the pre and post-collapse equilibrium paths and we perform parametric studies in order to investigate the significance of the different geometrical imperfections and of the residual stresses on the collapse and collapse propagation pressures.

The finite element models were developed using the nonlinear shell elements in the general-purpose finite element code ADINA [19]. The main features of the finite element models are:

- MITC4 shell element (4-node element that includes shear deformations) [20-22].
- Automatic solution of the incremental nonlinear finite element equations [13].
- Material nonlinearity: elasto-plastic material model [12],
    - ✓ Von Mises associated plasticity.
    - ✓ Isotropic hardening.
- Geometrical nonlinearity: large displacements / rotations [12, 23].
- For the cases with external pressure plus bending we first impose the bending and then the external pressure keeping constant the imposed curvature.

In order to validate the infinite tube finite element model, we consider a pipe under external pressure and in Fig. 17 we compare our results with the results published by Kyriakides in Ref. [10].

3.2. Infinite tube: finite element results

We investigate, using the finite element models we described above, the behavior of a typical steel seamless pipe (*D=8 5/8", t=12.7mm;* $\sigma_y = 60$ *kpsi*) under external pressure and bending.

Once the equilibrium path that describes the pre and post-collapse regimes has been determined, the collapse propagation pressure can be calculated using Maxwell's construction [10].

3.2.1. Effect of the pipes ovality

Even tough the pipes initial ovality has a strong influence on the pipes critical collapse pressure when no bending is applied [9], the effect of the initial ovality on the pipes critical collapse pressure diminishes when the imposed curvature is increased (see Fig. 18). When a perfectly round tube is bended the cross section is ovalized (*"Brazier effect"*), when the bending increases, the Brazier-ovality grows and therefore the pipes initial ovality becomes less important as compared with this bending-induced ovality.

In Fig. 18 we measure the applied curvature with the radius *"R"* and with the maximum bending strain (as a reference we have indicated the radius of a typical reel used to lay marine pipelines).

The effect of the pipe initial ovalities on their collapse propagation pressure is negligible for any bending situation, as shown in Fig. 19.

It is important to remark that in our analyses when we refer to initial ovality we refer to the value of the second mode in a Fourier series analysis of the OD shape, which is measured with our "shape-meter", as shown in Fig. 20. A detailed description of our "shape-meter" is presented in Ref. [9].

The value of that second mode is quite different (lower) from the ovality measured with a standard API ovalimeter, which is an electronic caliper that it is used at any section to measure the maximum and minimum diameters, so as to calculate the ovality as,

$$Ov = \frac{D_{\max} - D_{\min}}{D_{average}} \tag{2}$$

In Fig. 21 we show a typical example [24].

3.2.2. Effect of the pipes eccentricity

For low values of applied bending the eccentricity effect on the pipes collapse pressure is much lower than the ovality effect, and it is almost independent of the applied bending (Fig. 22).

The eccentricity effect on the pipes collapse propagation pressure is not very relevant (Fig. 23).

3.2.3. Effect of the residual stresses

In Figs. 24 and 25 we present the effect of the residual stresses on the pipes collapse pressure and collapse propagation pressure, for various values of imposed bending (the bending is measured, in these figures, with the relation between the imposed curvature and the curvature that yields the most strained fiber of the pipe section: k/k_y).

The effect of the residual stresses on the pipes external collapse pressure depends on the applied bending. For the lower values of curvature, the external collapse pressure decreases when the residual stresses absolute value increases, but for higher bending the collapse pressure increases when the residual stresses change from negative to positive values. The effect of the residual stresses on the pipes critical collapse pressure is quite low when a strong bending is applied.

The effect of the residual stresses on the pipes collapse propagation pressures is not very important, with or without bending.

3.2.4. Effect of the imposed bending

As it can be seen in the above figures bending diminishes the external collapse pressure of the pipes, due to the fact that it increases its ovality.

It is also interesting to observe that bending increases the pipes collapse propagation pressure.

3.3. Finite tube: finite element results

In Ref. [9] we analyzed the collapse of short (finite) samples under external pressure only and we compared the finite element solutions with experimental results, obtaining a very good validation for the collapse pressure numerical predictions.

In the previous sub-section we determined the collapse and collapse propagation pressures of long (infinite) samples under external pressure plus bending. In this sub-section we investigate, using also shell finite element models, the pre and post-collapse regimes of short (finite) sample under external pressure. We analyze the same seamless steel pipe that we investigated previously (*D=8 5/8", t=12.7mm;* $\sigma_y = 60$ *kpsi*), but we consider a finite sample with a length of 6 meters and its ends prevented from in-plane deformation. We added contact surfaces [12] on the pipe intrados to avoid the interpenetration of the pipe walls.

In Fig. 26 we display the pre and post-collapse equilibrium path of a pipe with an initial ovality of 0.3% and the finite element meshes corresponding to various stages along the equilibrium path. In Fig. 27 we present the sequential deformation of a pipe generator indicating the collapse propagation. Finally in Fig. 28 we compare the finite element and experimentally determined buckled shapes close to one of the pipe ends.

4. Conclusions

In this paper we discussed the finite element models that we developed for simulating the service performance of the tubular steel products used in the oil industry. These tubular products include the oil country tubular goods (OCTG), that is to say the tubular products used in the oil wells, and the pipes used in pipeline applications.

In the case of the analysis of OCTG threaded connections, the finite element models are used to analyze alternative designs and rank them regarding their structural and sealing performances.

The analysis of the effect of pipes imperfections on the collapse behavior of tubes enables the definition of geometrical and mechanical manufacturing tolerances.

Since important technological decisions are reached based on the results provided by finite element models, it is of utmost importance the reliability of these results. In this paper we also discussed the reliability requirements that we impose on finite element formulations.

Acknowledgements

We gratefully acknowledge the support of the TENARIS group for this research.

5. References

1. American Petroleum Institute, Standard API5B.
2. A.P.Assanelli, K.Xu, F.Benedetto, D.H.Johnson and E.N.Dvorkin, "Numerical / experimental analysis of an API 8-round connection", *ASME, J. Energy Resources Technology*, Vol.119, pp.81-88, 1997.
3. A.P.Assanelli and E.N.Dvorkin, "Selection of an adequate element formulation for modeling OCTG connections", *Computational Mechanics – New trends and applications*, (Ed. S.Idelsohn et al), CIMNE, 1998.
4. A.P.Assanelli and E.N.Dvorkin, "Finite element models of OCTG threaded connections", *Computers & Structures*, Vol.47, pp.725-734, 1993.
5. E.N.Dvorkin, A.P.Assanelli and R.G.Toscano, "Performance of the QMITC element in 2D elasto-plastic analyses", *Computers & Structures*, Vol.58, pp.1099-1129, 1996.
6. E.N.Dvorkin and R.G.Toscano, "Effects of external/internal pressure on the global buckling of pipelines", *Computational Fluid and Solid Mechanics – Proceedings First MIT Conference on Computational Fluid and Solid Mechanics*, (Ed. K.-J. Bathe), Elsevier, 2001.
7. A.C. Palmer, "Lateral Buckling of Axially Constrained Pipelines", *JPT Forum*, 1974.

8. A.C. Palmer and J.H. Martin, “Buckle propagation in submarine pipelines”, *Nature*, Vol. 254, 46-48 (1975).
9. A.P.Assanelli, R.G.Toscano, D.H.Johnson and E.N.Dvorkin, “Experimental / numerical analysis of the collapse behavior of steel pipes”, *Engng. Computations*, Vol.17, pp.459-486, 2000.
10. S. Kyriakides, “Propagating instabilities in structures”, *Advances in Applied Mechanics*, Vol. 30, pp. 67-189, 1994.
11. R.G.Toscano, M.P.Amenta and E.N.Dvorkin, **“**Enhancement of the collapse resistance of tubular products for deep-water pipeline applications”, *Proceedings Offshore Pipeline Technology Conference*, Amsterdam, 2002.
12. K.J. Bathe, *Finite Element Procedures*, Prentice Hall, NJ, 1996.
13. K.J. Bathe and E.N. Dvorkin, "On the automatic solution of nonlinear finite element equations", *Computers & Structures*, Vol. 17, pp. 871-879, 1983.
14. E.N.Dvorkin and S.I.Vassolo, "A quadrilateral 2D finite element based on mixed interpolation of tensorial components", *Engng. Computations*, Vol.6, pp.217-224, 1989.
15. E.N.Dvorkin, D.Pantuso and E.A.Repetto, "A finite element formulation for finite strain elasto-plastic analysis based on mixed interpolation of tensorial components", *Comput. Meth. Appl. Mechs. Engng*., Vol.114, pp.34-54, 1994.
16. O.C.Zienkiewicz and R.L.Taylor, *The Finite Element Method*, Fourth edition, McGraw-Hill (U.K.), 1989.
17. E.N.Dvorkin, “On the convergence of incompressible finite element formulations: the Patch Test and the Inf-Sup condition", *Engng. Computations*, Vol.18, pp.539-556, 2001.
18. R.H.MacNeal, “A theorem regarding the locking of four-noded membrane elements”, *Int. J. Num. Meth. Engng.*, Vol.24, pp.1793-1799, 1987.
19. The ADINA System, ADINA R&D, Watertown, MA, USA.
20. E.N. Dvorkin and K.J. Bathe, "A continuum mechanics based four-node shell element for general nonlinear analysis", *Engng. Computations*, Vol. 1, pp. 77-88, 1984.
21. K.J. Bathe and E.N. Dvorkin, "A four-node plate bending element based on Mindlin / Reissner plate theory and a mixed interpolation", *Int. J. Numerical Methods in Engng*., Vol. 21, pp. 367-383, 1985.
22. K.J. Bathe and E.N. Dvorkin, "A formulation of general shell elements - the use of mixed interpolation of tensorial components", *Int. J. Numerical Methods in Engng*., Vol. 22, pp. 697-722, 1986.
23. E.N.Dvorkin, E.Oñate and J.Oliver, "On a nonlinear formulation for curved Timoshenko beam elements considering large displacement/rotation increments", *Int. J. Numerical Methods in Engng*., Vol. 26, pp. 1597-1613, 1988.
24. A.P. Assanelli and G. López Turconi, “Effect of measurement procedures on estimating geometrical parameters of pipes”, *2001 Offshore Technology Conference*, Paper OTC 13051, Houston, Texas, 2001.

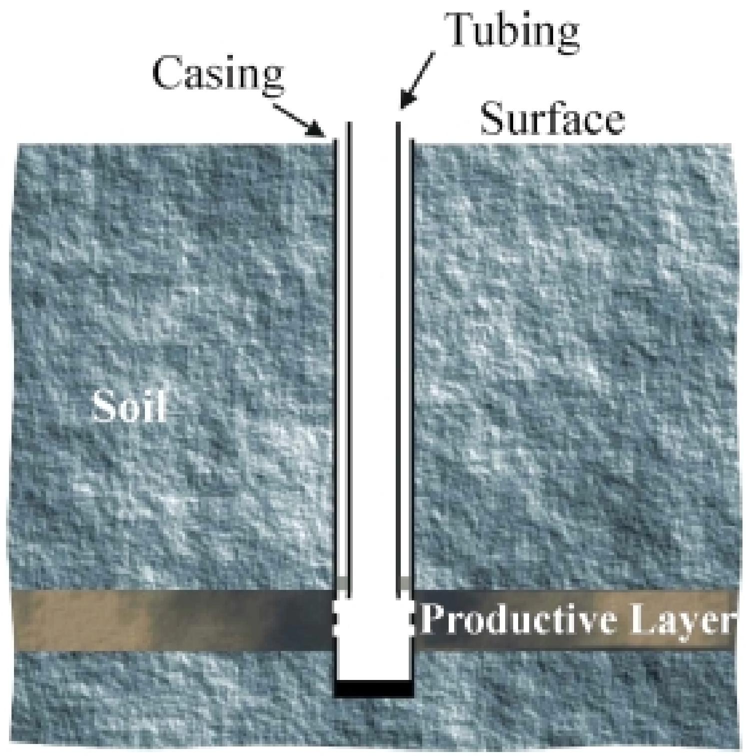

Figure 1. Steel tubes (casing and tubing) in an oil well

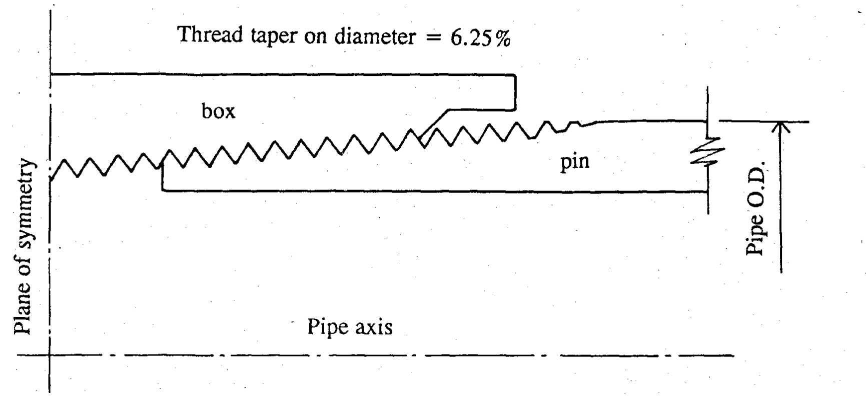

(a) API 8-Round Connection

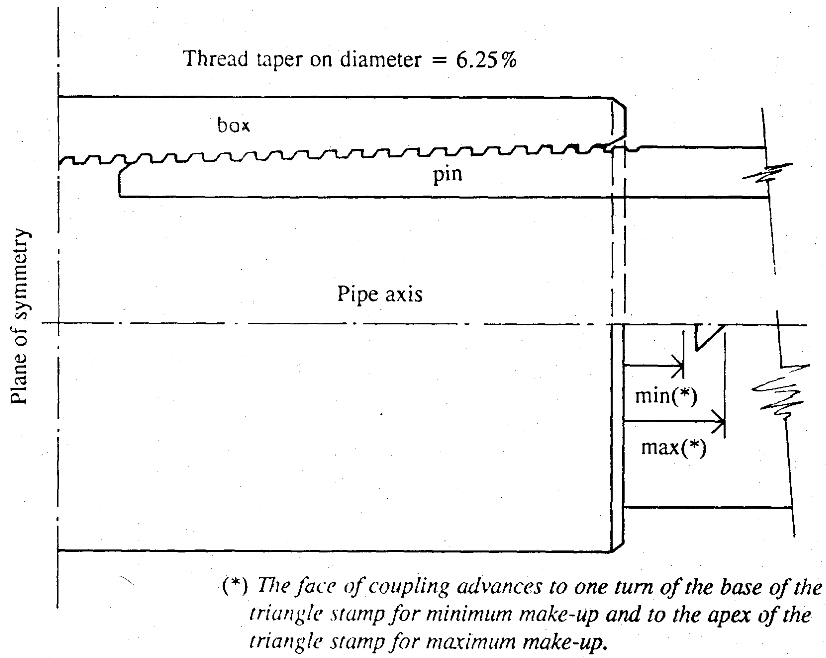

(b) API Buttress connection

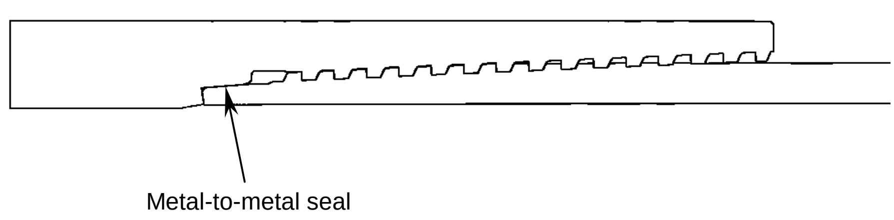

(c) Premium connection

Figure 2. API and premium connections

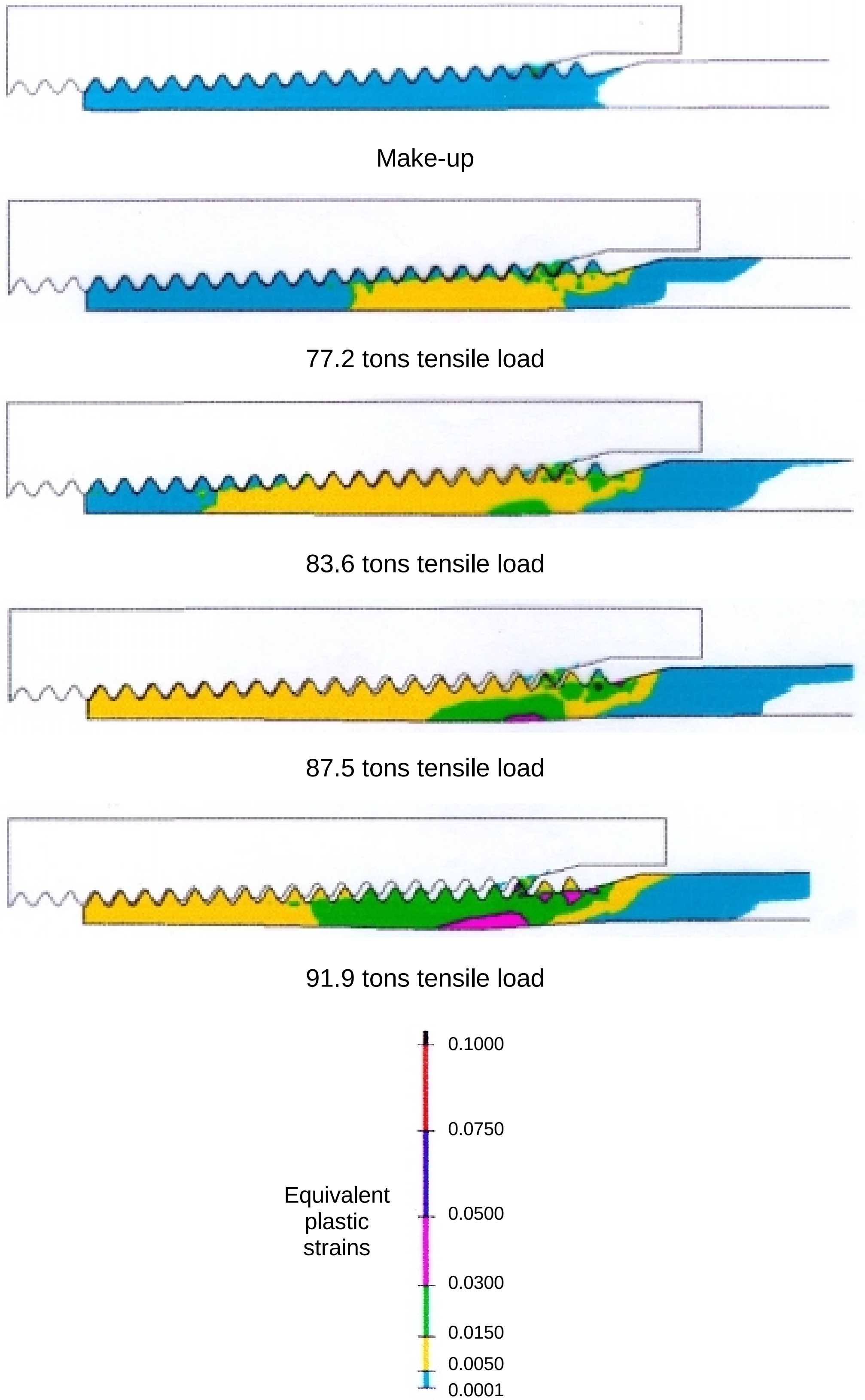

Figure 3. Jump-out of an API 8R connection

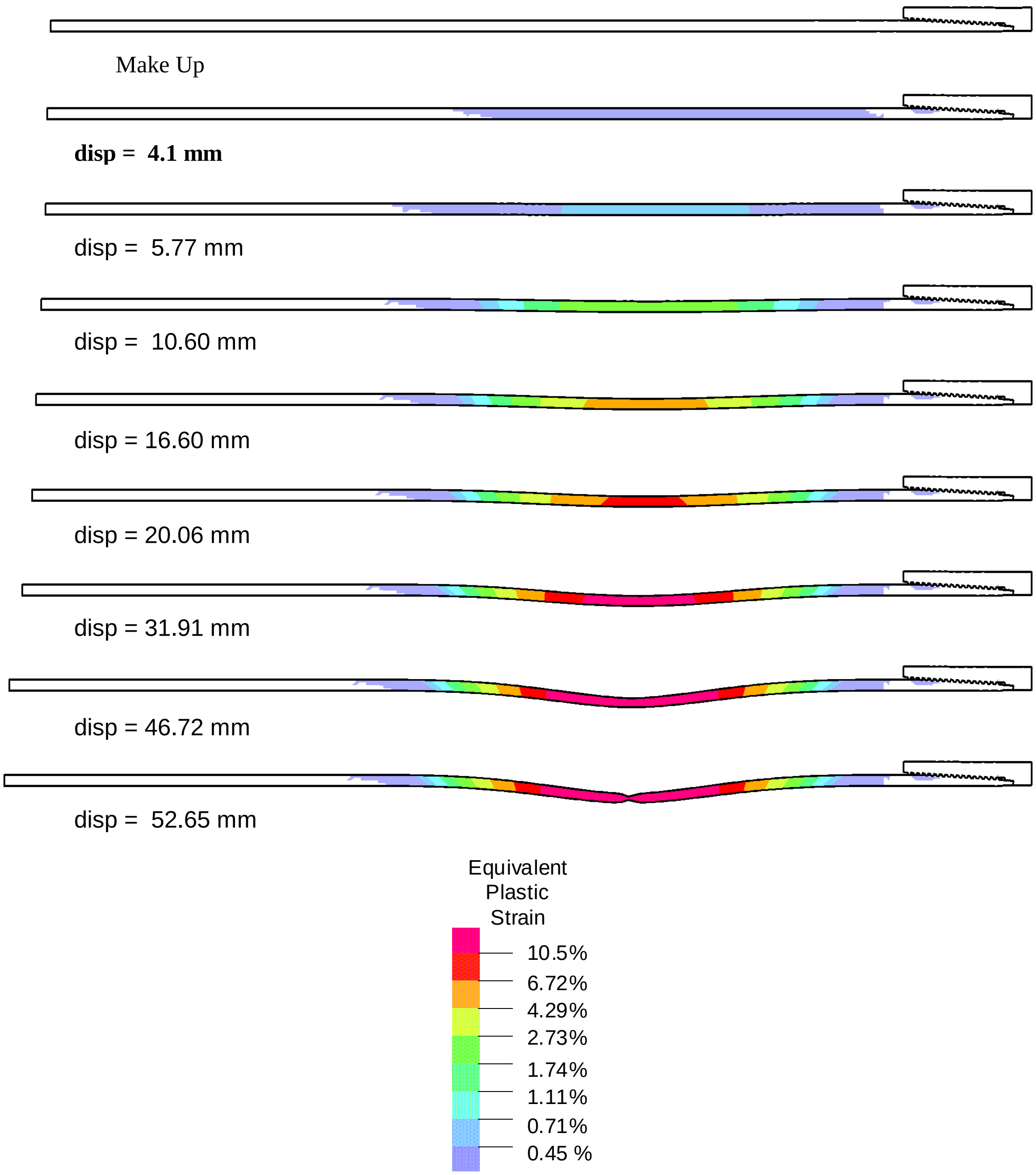

Figure 4. Finite element simulation of necking in a premium connection

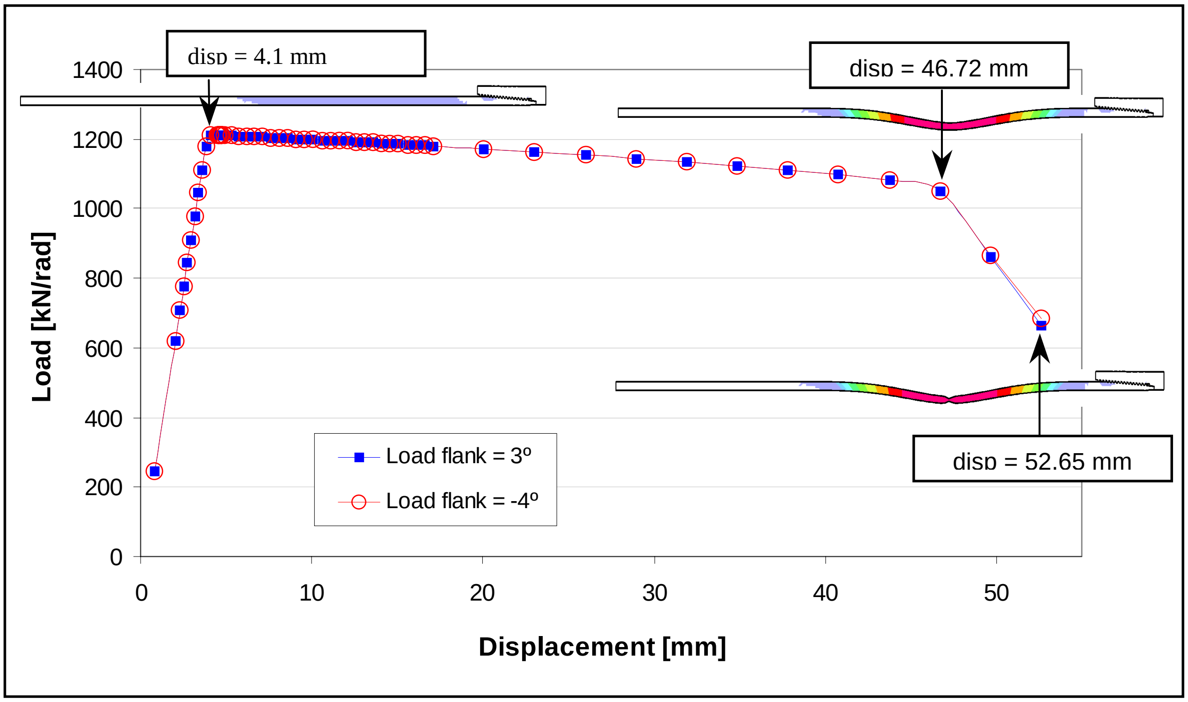

Figure 4 (continued)

Figure 5. Rupture of the pipe material without the development of large plastic strains

Figure 6. Localized collapse

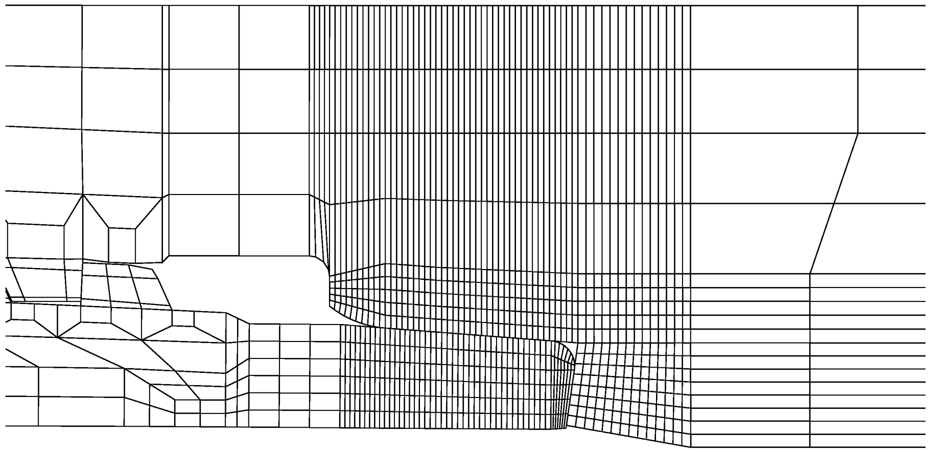

Figure 7. Typical mesh with distorted elements

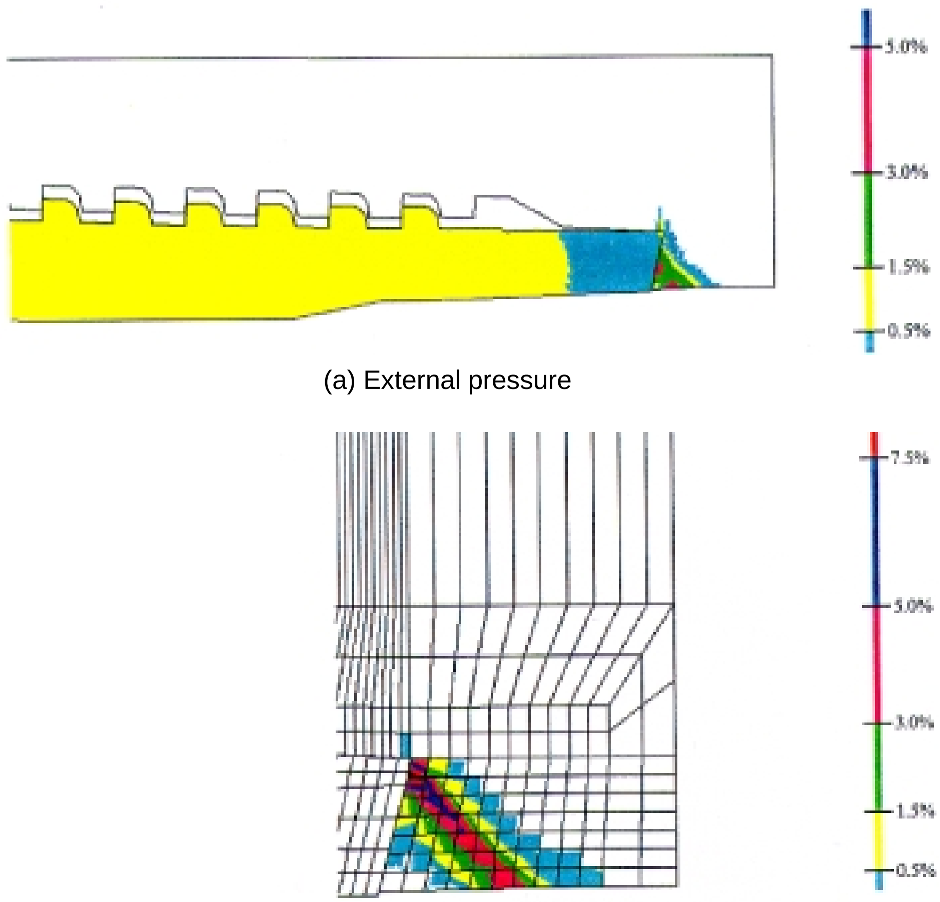

(a) External pressure

(b) Overtorque

Equivalent plastic strains

Figure 8. Shear bands in the connection coupling

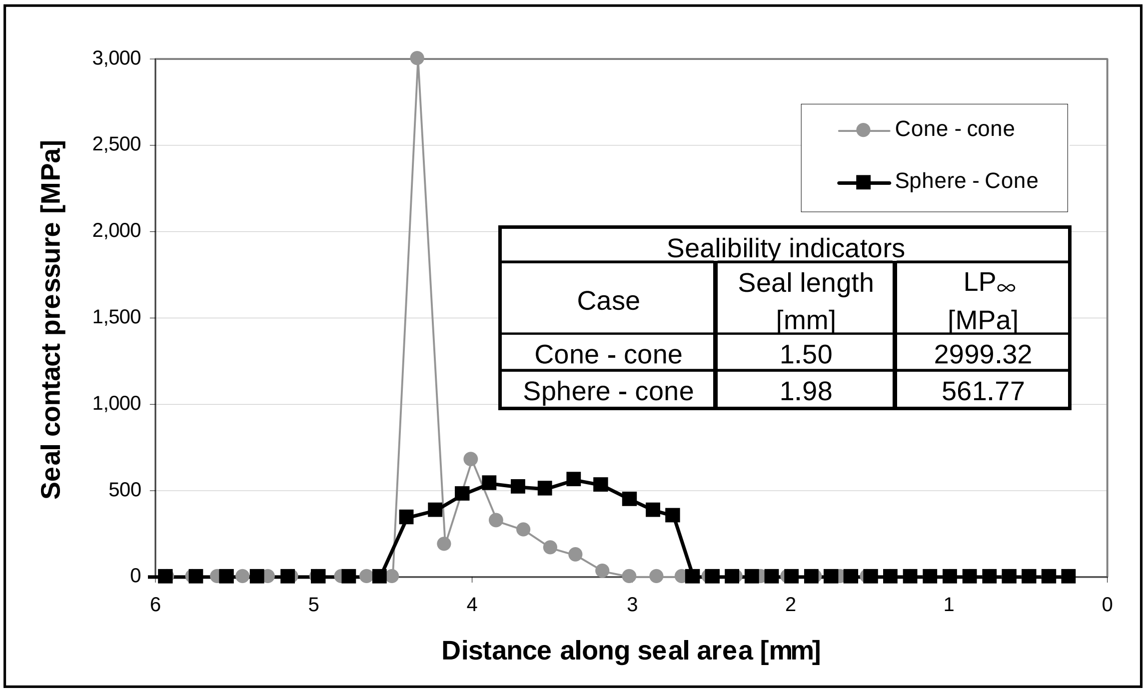

Sealibility indicators		
Case	Seal length [mm]	LP_∞ [MPa]
Cone - cone	1.50	2999.32
Sphere - cone	1.98	561.77

Figure 9. Cone-to-cone and sphere-to-cone metal-to-metal seals

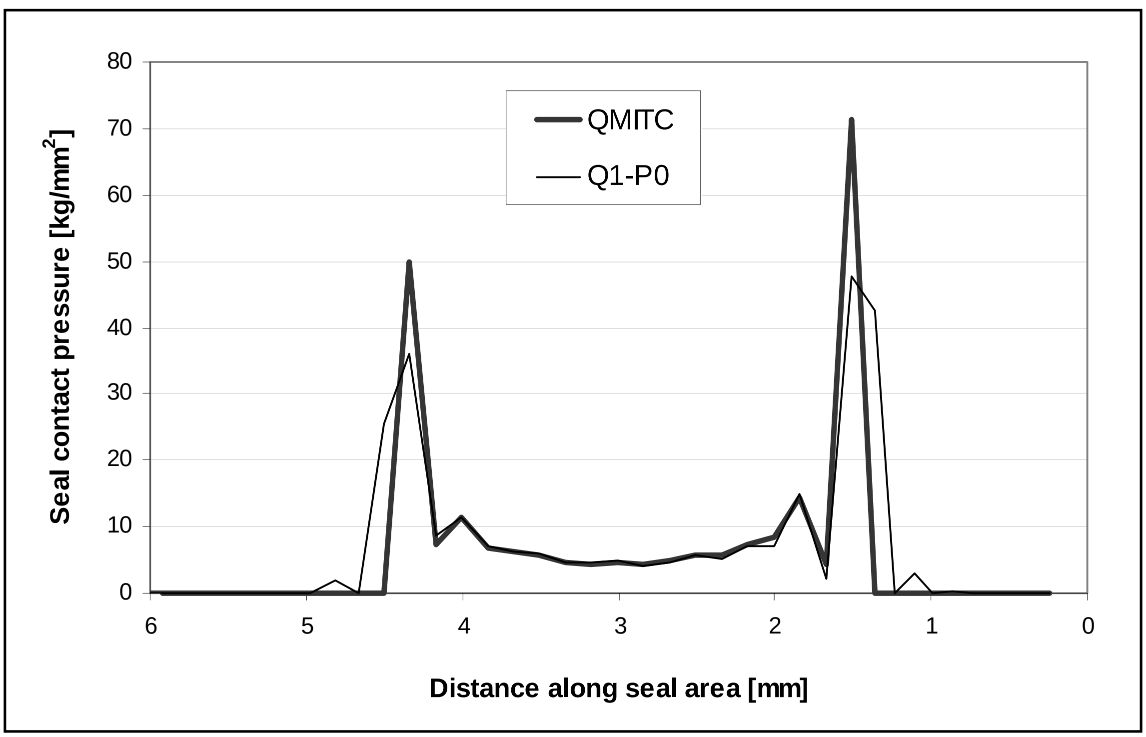

Figure 10. Comparison of different element predictions

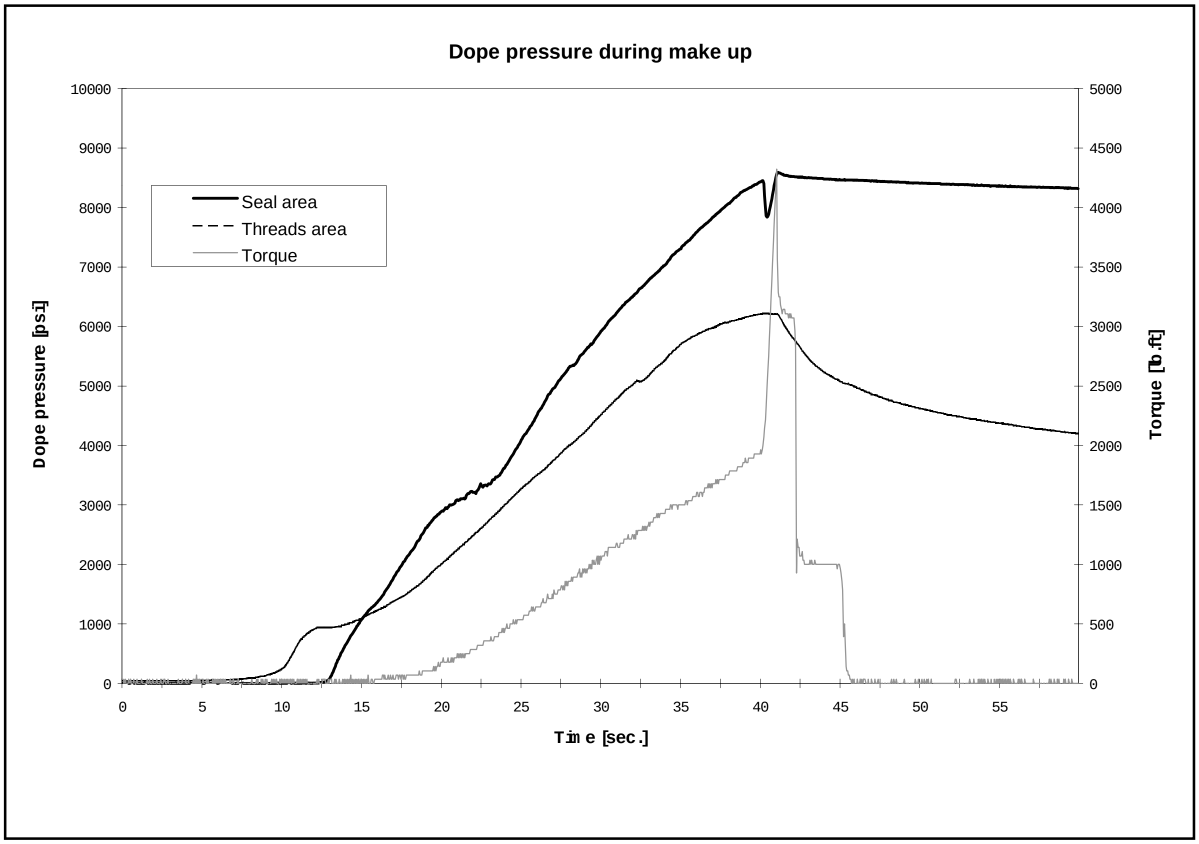

Figure 11. Dope pressure values

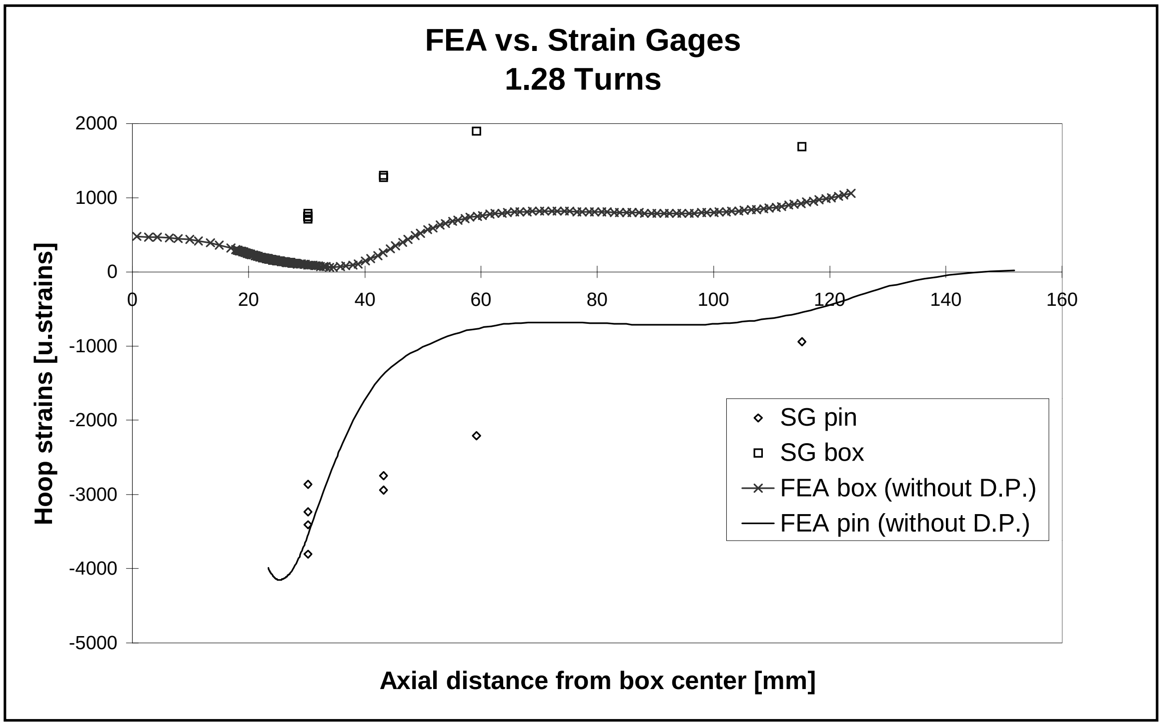

Figure 12. Strains comparison without considering dope pressure in an over-doped connection

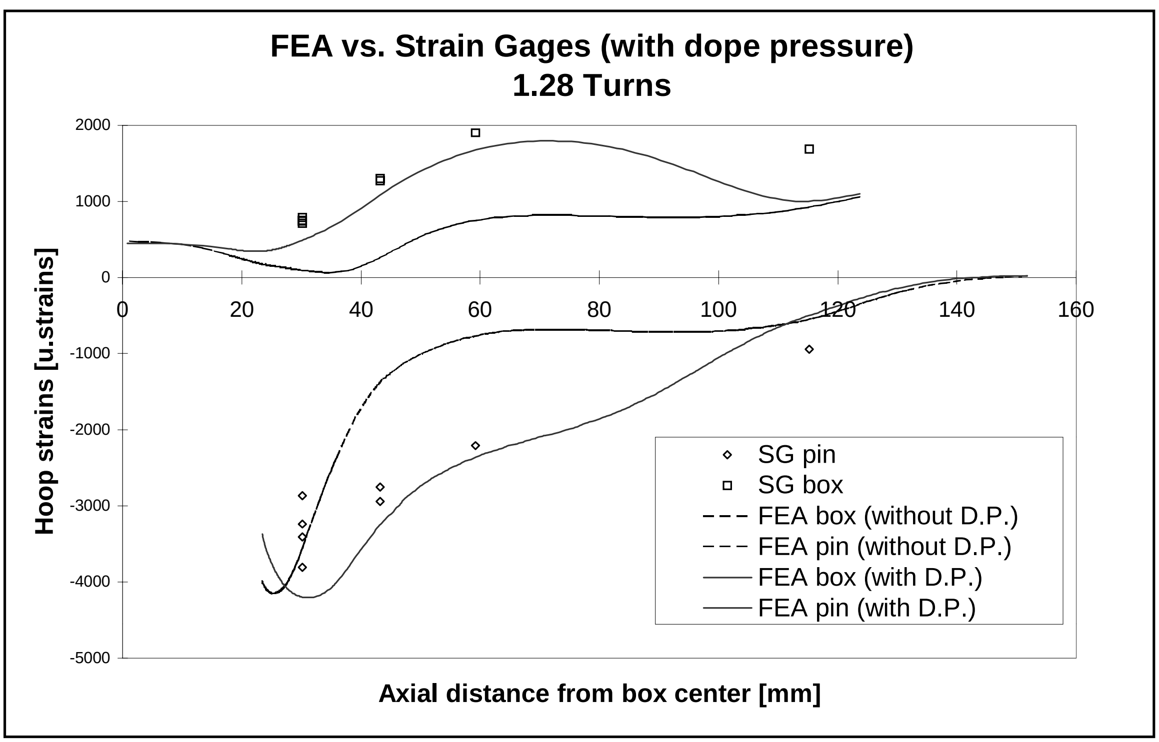

Figure 13. Finite element analysis considering dope pressure

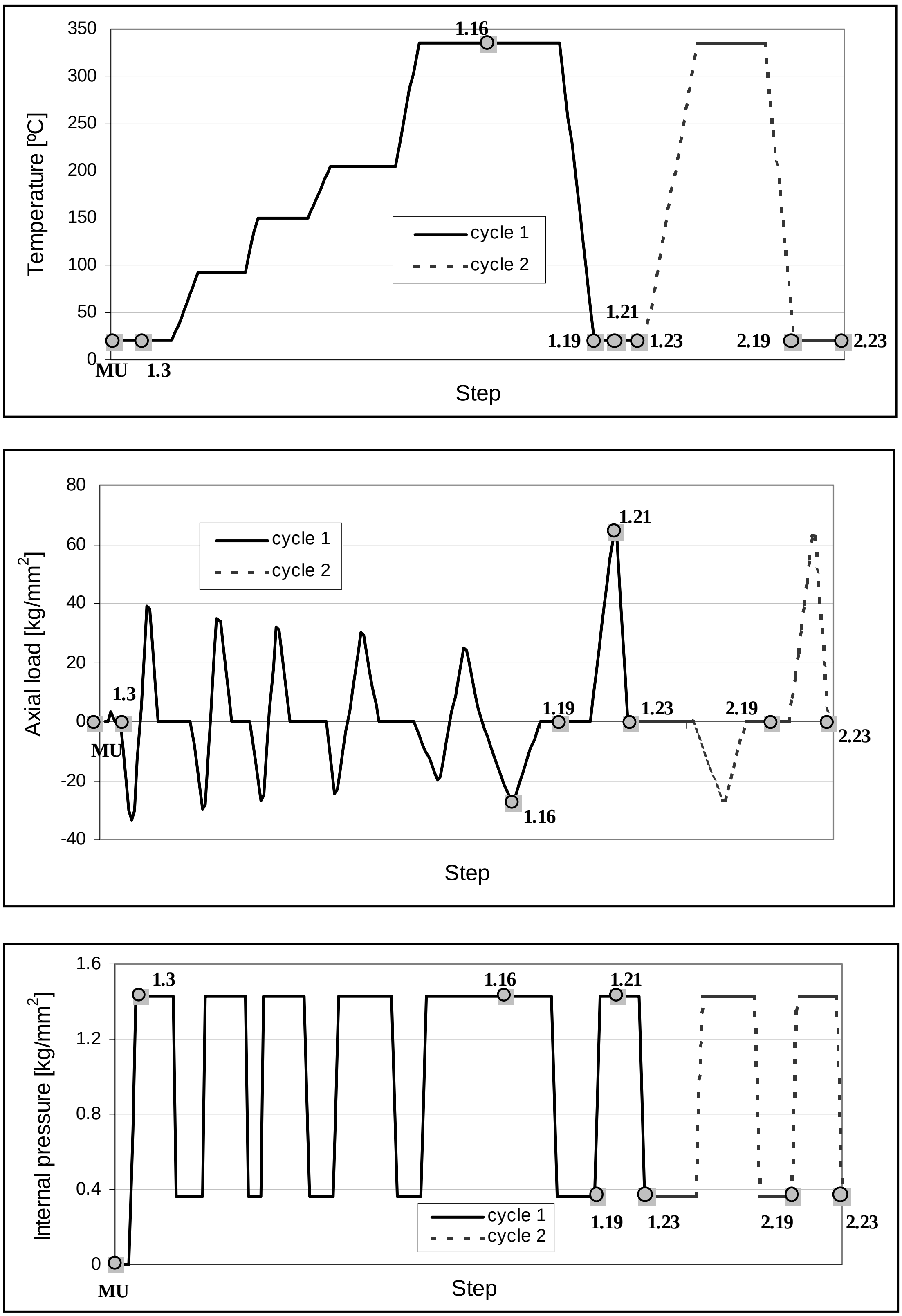

Figure 14. Steam injection string: Thermal and mechanical loads

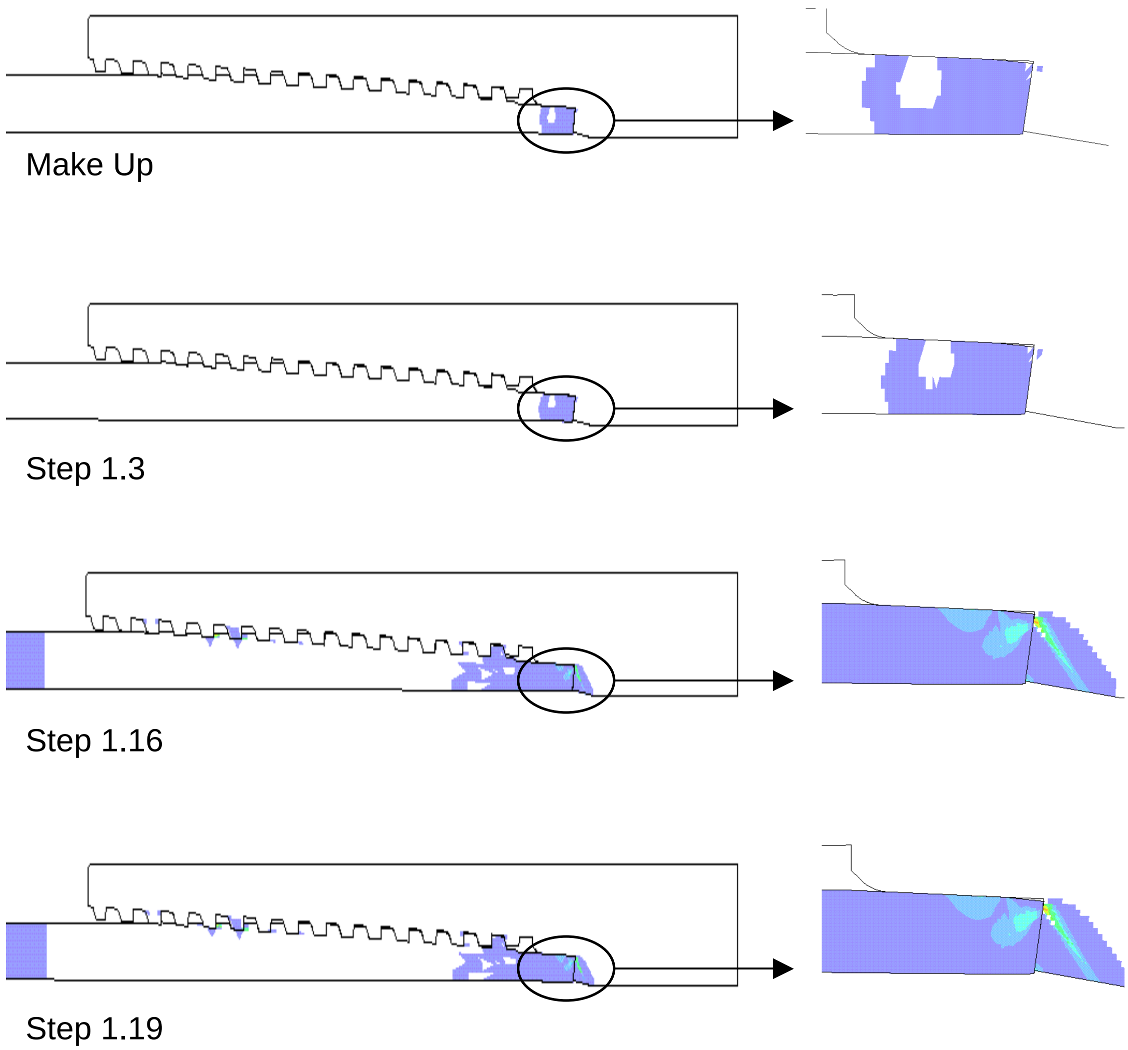

Step	Axial load	strain	Temp.	Inside pressure	Yield Tension
	kg/mm2	micro-strain	ºC	kg/mm2	kg/mm2
Make Up	0.0		20	0	59.23
1.3	0.0		20	1.43	59.23
1.16	resultant	-400	336	1.43	35.9
1.19	0.0		20	0.36	59.23

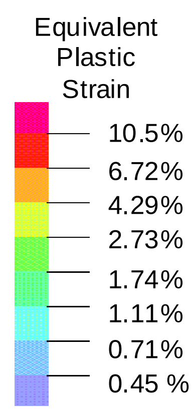

Figure 15. Steam injection string: Finite element results

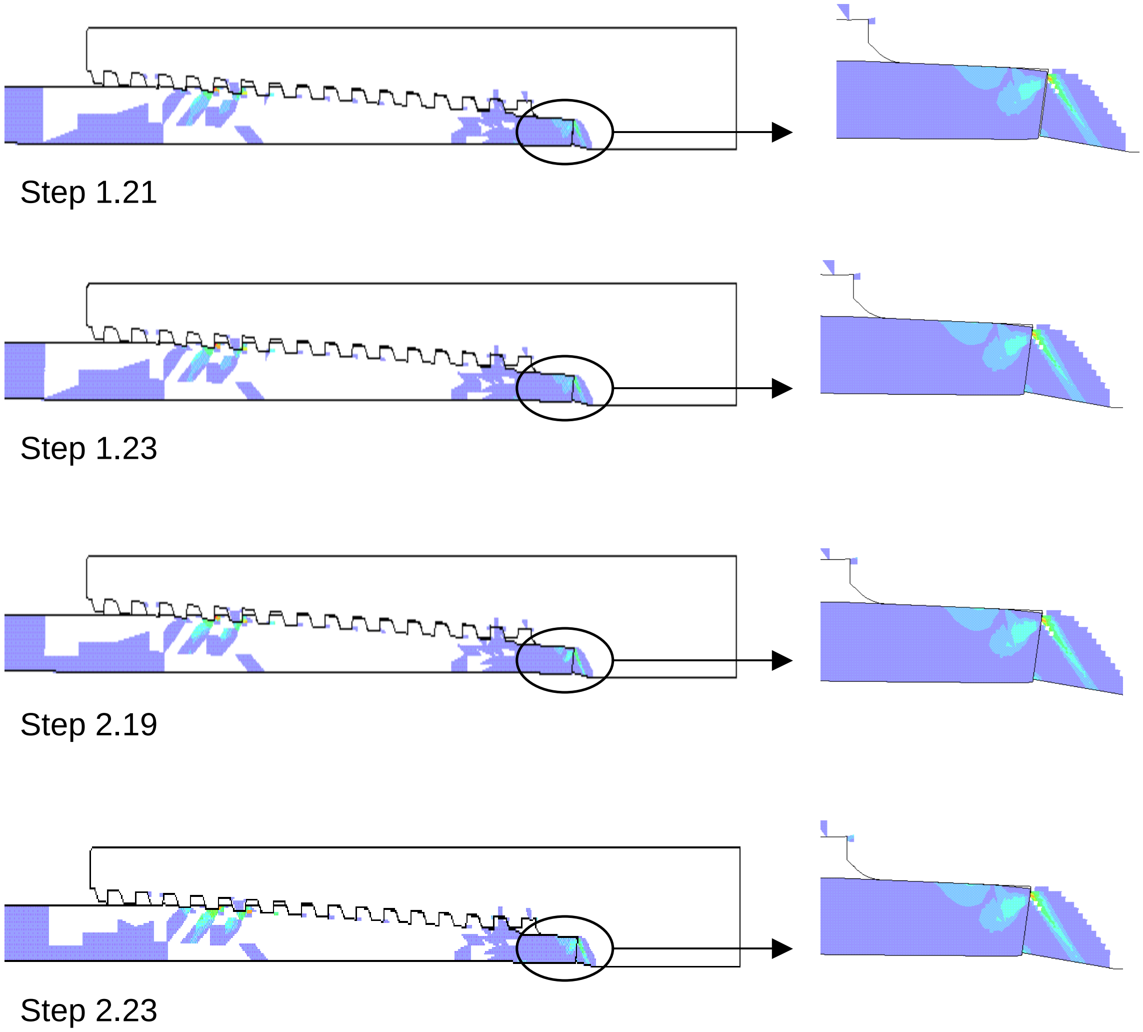

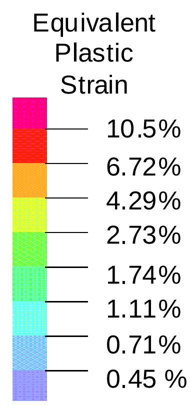

Step	*Axial load*	*strain*	*Temp.*	*Inside pressure*	*Yield Tension*
	kg/mm2	micro-strain	ºC	kg/mm2	kg/mm2
1.21	resultant	0.0	20	1.43	59.23
1.23	0.0		20	0.36	59.23
2.19	0.0		20	0.36	59.23
2.23	0.0		20	0.36	59.23

Figure 15 (continued)

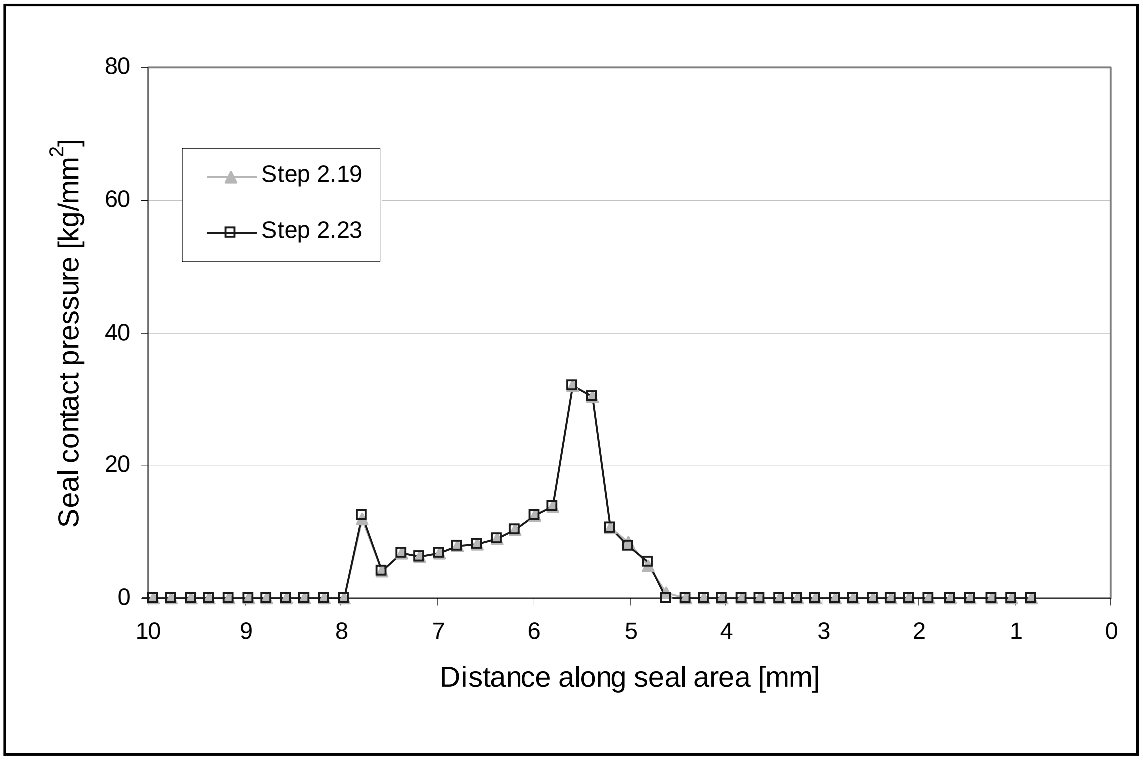

Figure 16. Seal contact pressure

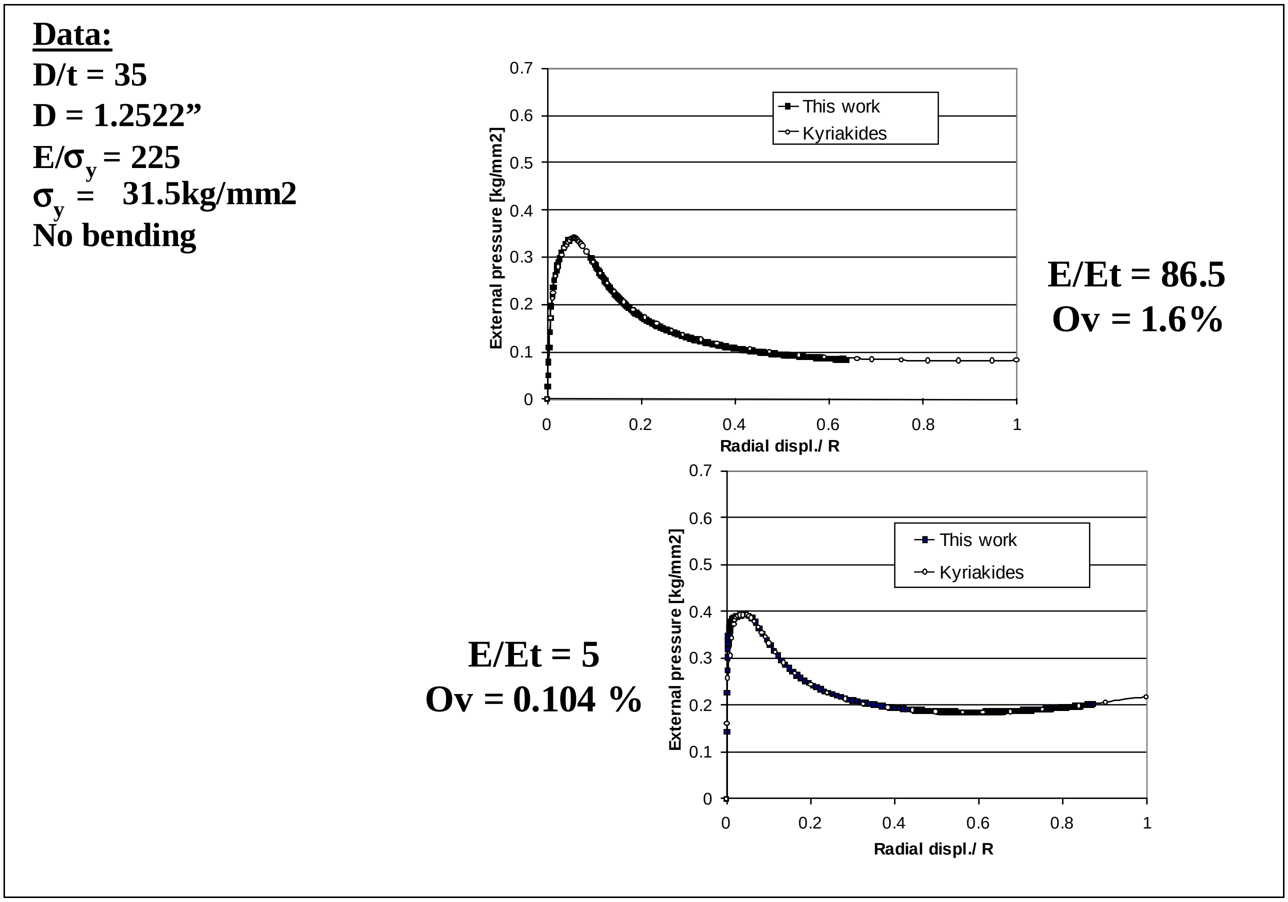

Figure 17. Infinite tube: qualification of the finite element model for the pre and post-collapse equilibrium path

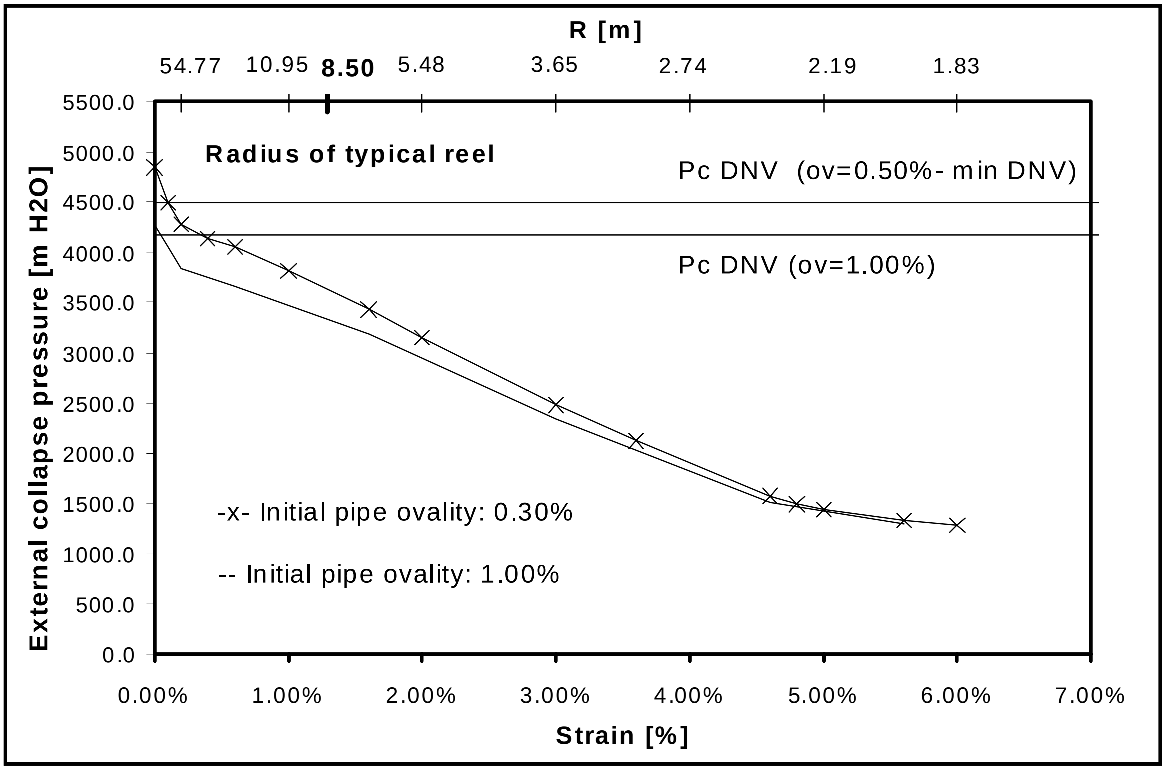

Figure 18. Infinite tube: ovality effect on the collapse pressure

(The values calculated with the DNV standard are presented here as a reference)

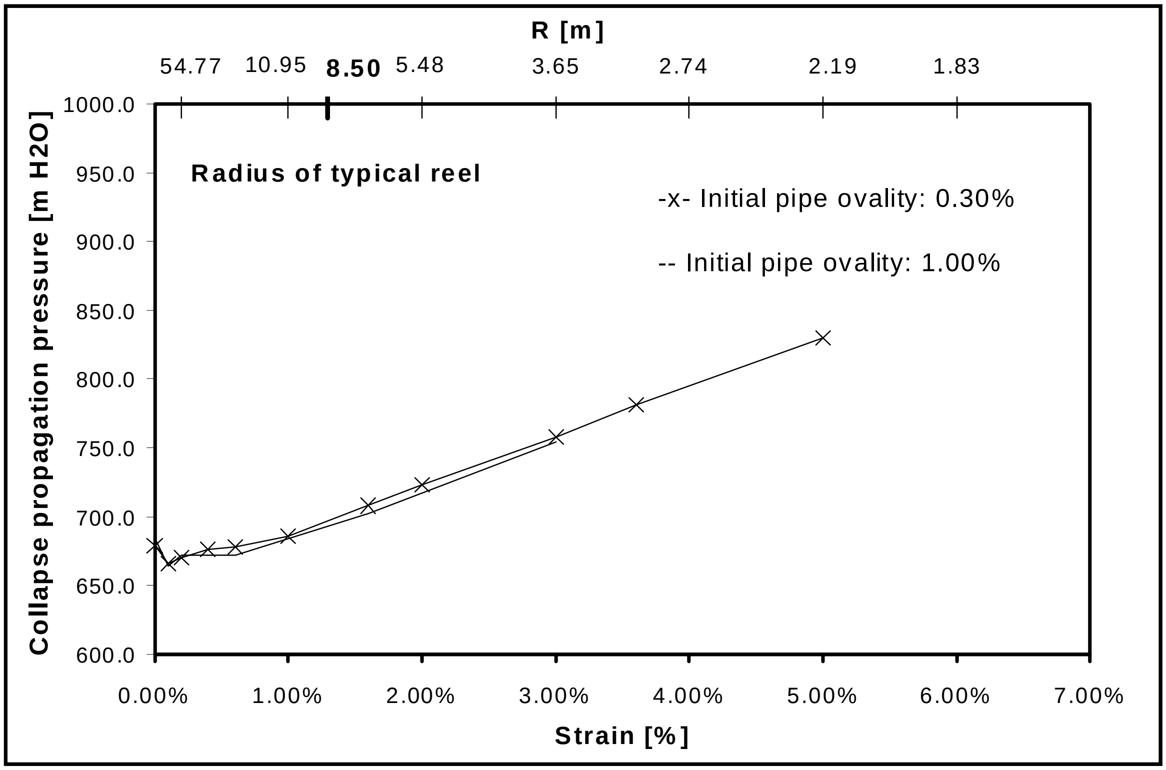

Figure 19. Infinite tube: ovality effect on the collapse propagation pressure

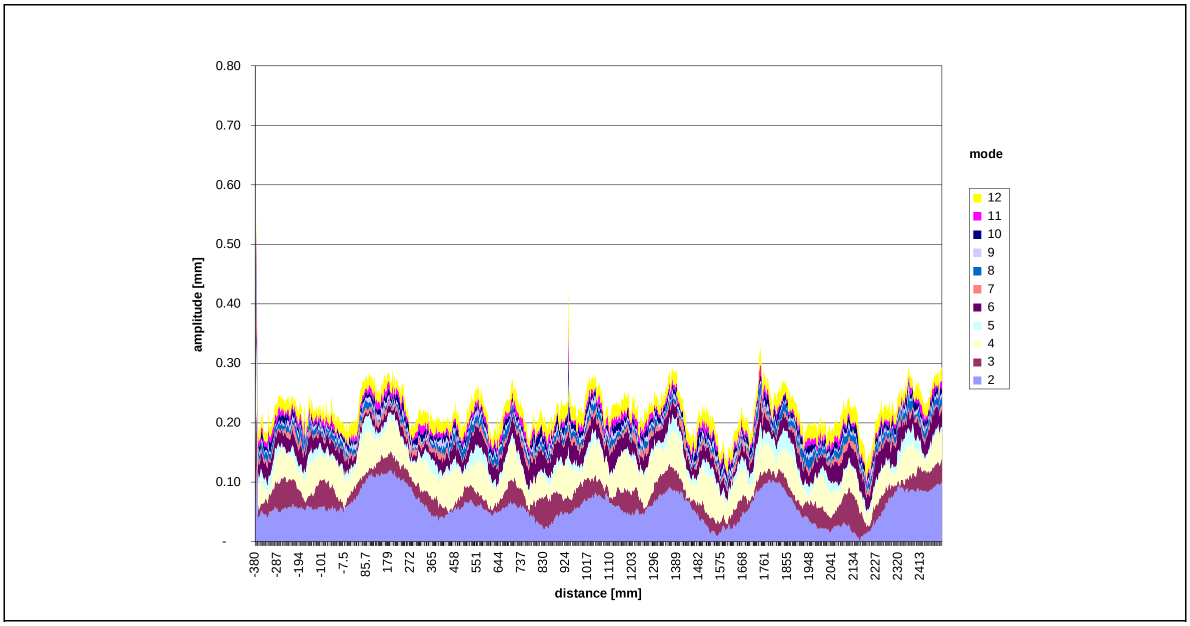

Figure 20. Fourier decomposition of the OD shape

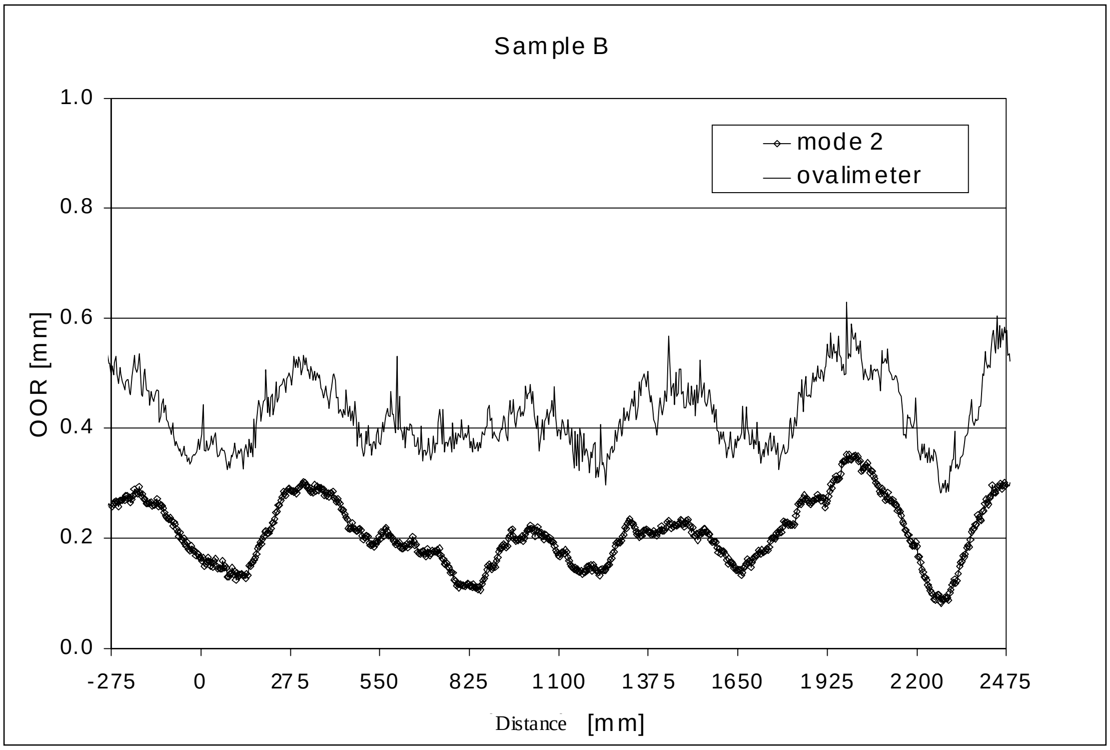

Figure 21. Comparison between *"mode 2"* and an API ovalimeter measurement

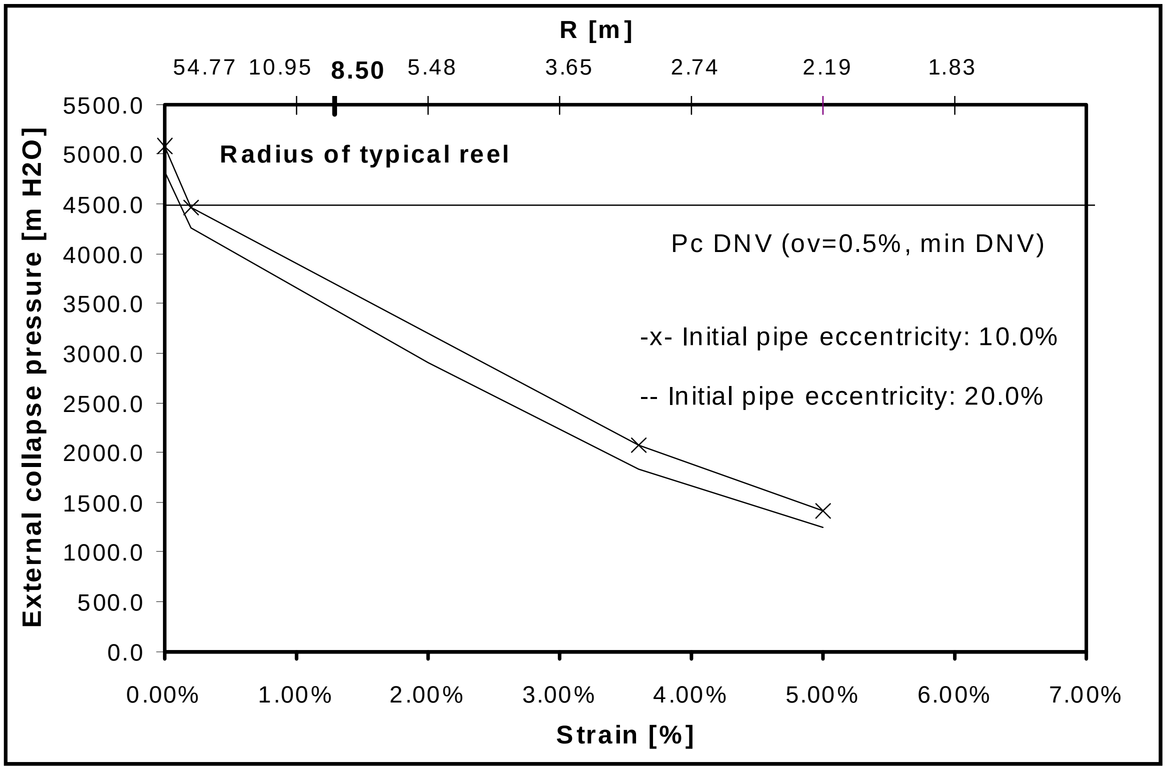

Figure 22. Infinite tube: eccentricity effect on the external collapse pressure

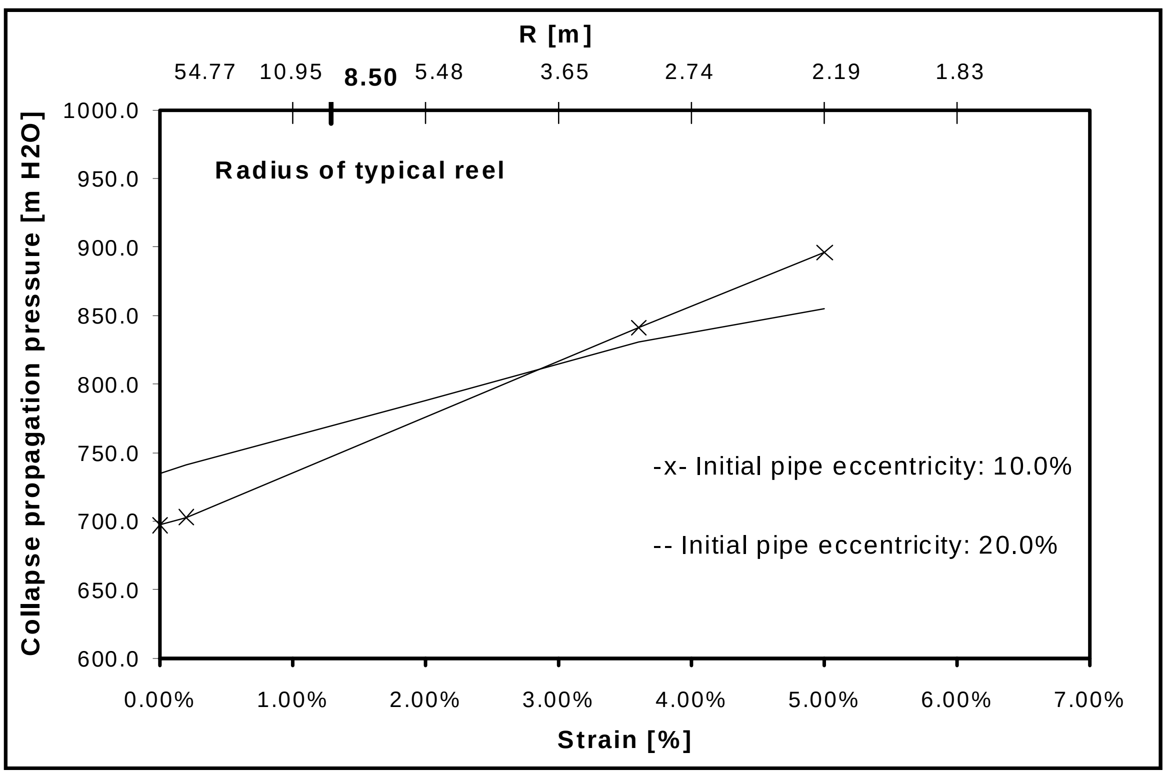

Figure 23. Infinite tube: eccentricity effect on the collapse propagation pressure

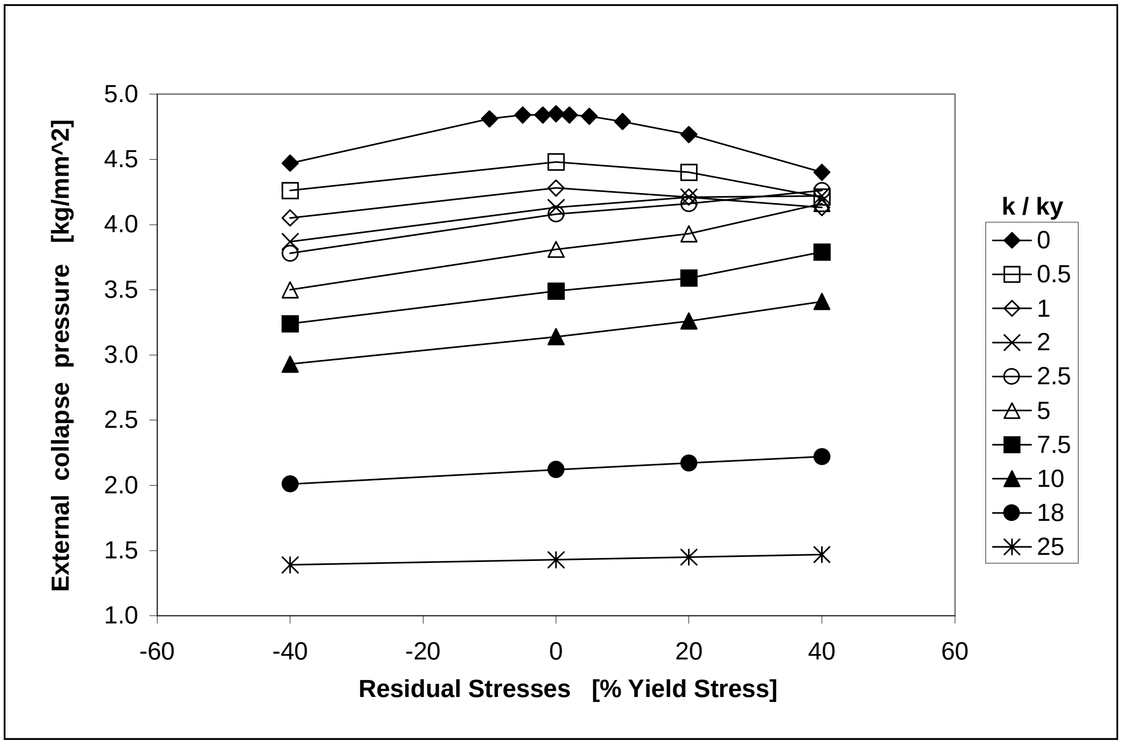

Figure 24. Infinite tube: residual stresses effect on the external collapse pressure
(RS>0 indicates compression at the inner radius)

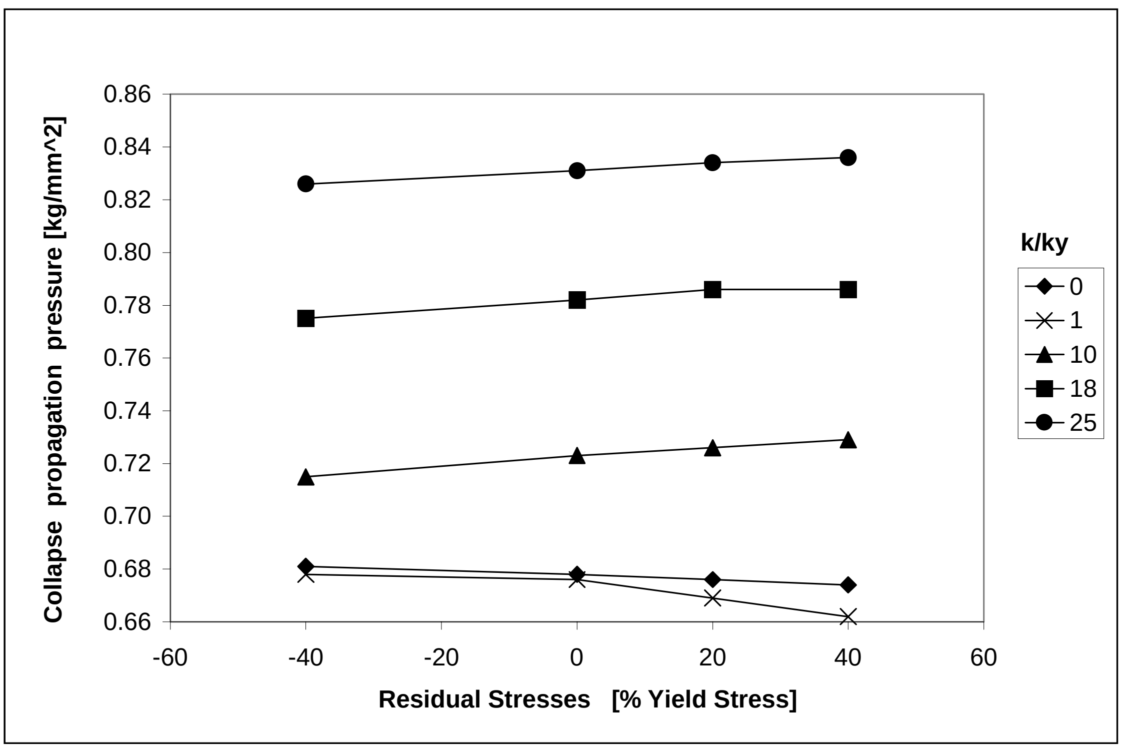

Figure 25. Infinite tube: residual stresses effect on the collapse propagation pressure

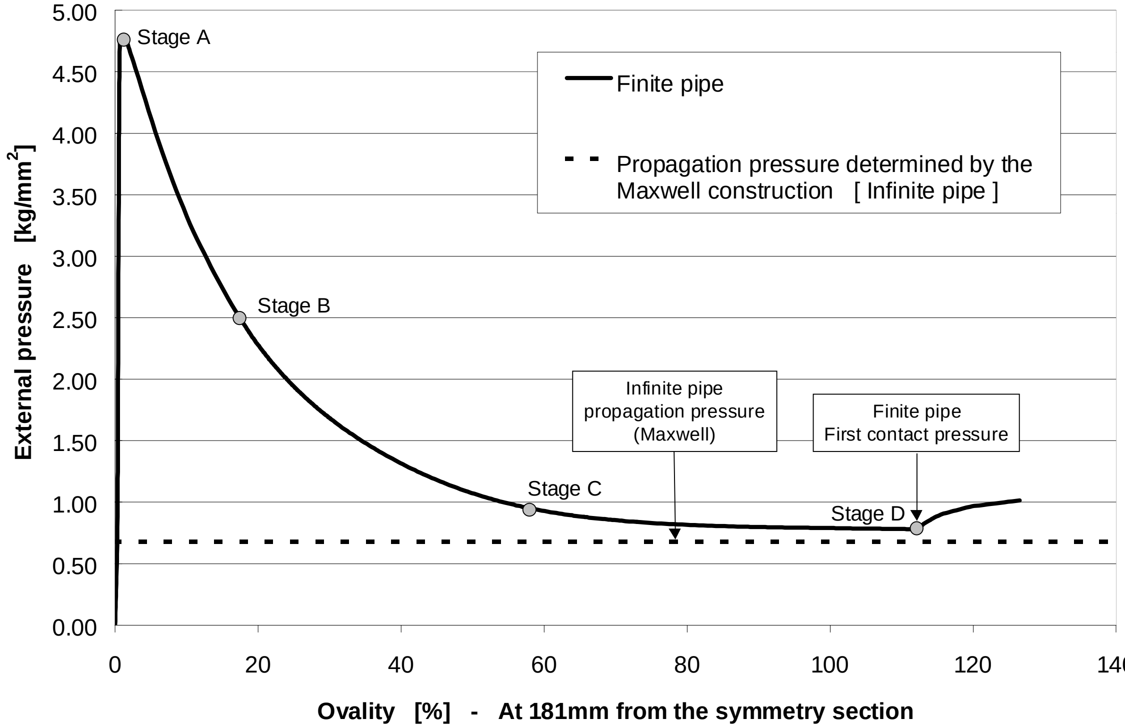

(a) Pre and post-collapse equilibrium path

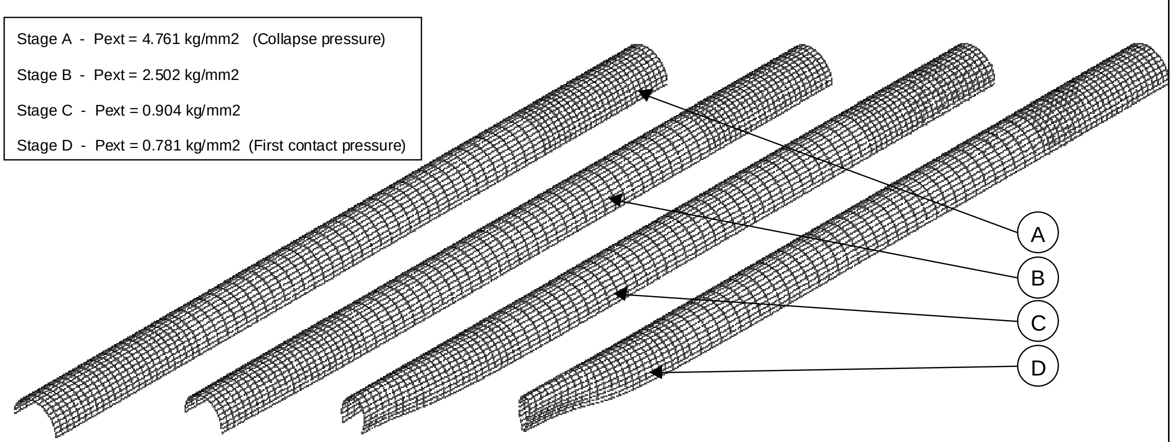

(b) Finite element meshes corresponding to four stages along the equilibrium path of the finite tube

Figure 26. Collapse of a finite tube

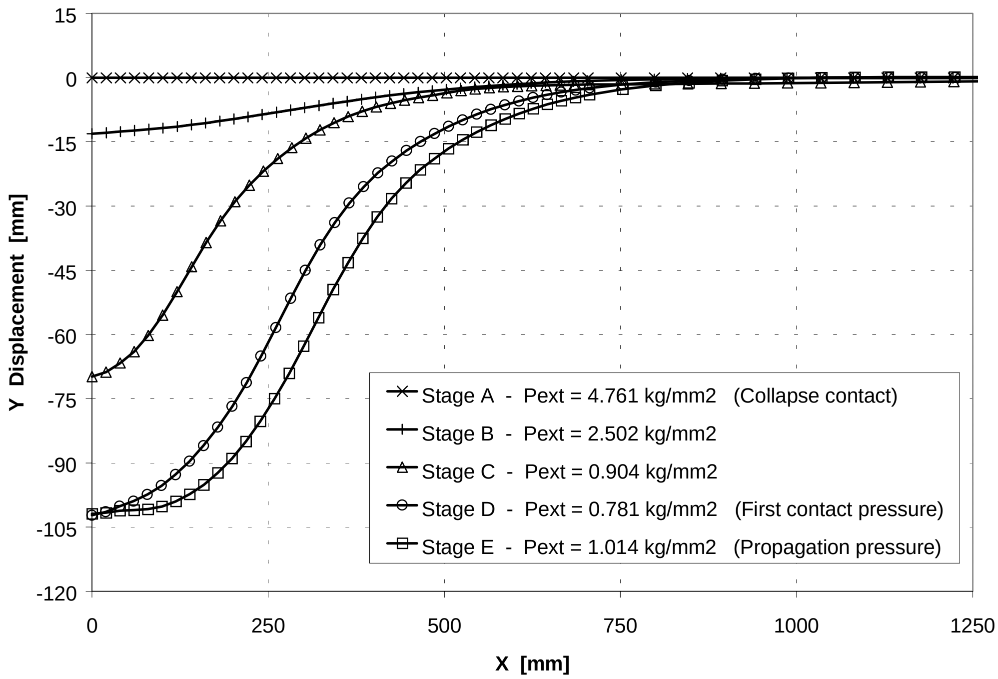

Figure 27. Finite tube: sequential deformation of a pipe generator

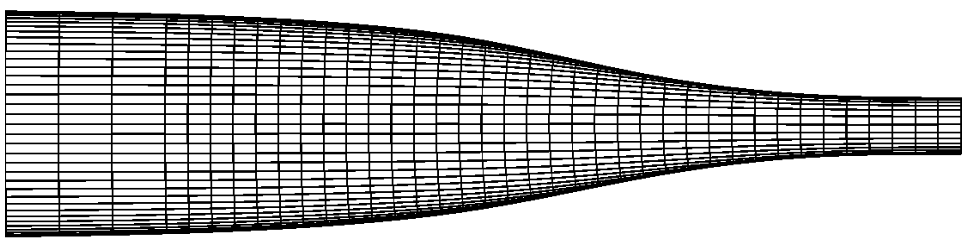

(a) Finite element buckled shape

(b) Experimental buckled shape

Figure 28. Comparison between finite element analysis and experimentally determined buckled shapes.